Environmental Earth Sciences (2023) 82:505
https://doi.org/10.1007/s12665-023-11180-y

ORIGINAL ARTICLE

Dolomitisation favoured by Lewis acidic background compounds in saline fluids

Veerle Vandeginste[1,2] · Elliot Hocknull[2] · Hossein Fazeli[3] · Yukun Ji[2,4]

Received: 1 October 2022 / Accepted: 6 September 2023 / Published online: 30 September 2023

Abstract

Predicting the type and rate of reactions between minerals and fluids is of utmost importance in many applications. Due to the presence of background ions, natural environments are often much more complex than laboratory experimental conditions that are used to derive mineral dissolution or precipitation rates. Dolomitisation is one of the most important diagenetic processes affecting carbonate rocks. Still, its underlying mechanisms are not yet completely unraveled. Here, we test the impact of background ions in saline solutions on the dolomitisation rate. Using batch reactor experiments at 200 °C and mineralogical characterisation, we demonstrate that the presence of background ions influences the fluid starting pH and specific ion effect, both impacting the dolomitisation rate. The results indicate that ions with a stronger hydration enthalpy correlate with a shorter dolomitisation induction time, and that Lewis acid $AlCl_3$ is more effective than Brønsted acid HCl. Importantly, dolomitisation occurred at a slightly acidic pH, and carbon speciation modelling showed that carbonate ions did not dominate in any of the experiments. Hence, dolomitisation in our experiments is faster in saline, slightly acidic rather than alkaline solutions and the rate is influenced by the solution composition, with specific ion effects influencing dolomite surface charge, interfacial tension and the structure of water. These new insights have implications for interpretations on natural environments, such as deep reservoirs with saline, slightly acidic formation water, and predictions related to geological carbon dioxide storage.

Keywords Dolomite · Alkalinity · Carbonate · Saline lake · Hydration enthalpy · Boehmite

Introduction

Understanding the type and rate of reactions between minerals and fluids is important for many applications, ranging from subsurface carbon storage to scaling of membranes in water treatment. Mineral dissolution or growth rates are obtained from laboratory experimental research, whereby well-defined, fairly simple chemical solutions are generally used. However, applying and upscaling those results for predictions in natural settings is challenging due to the chemical complexity, heterogeneity and hydrodynamic conditions of natural systems. Notably, the presence, concentration and type of background ions in solution can impact mineral dissolution and growth rates, as well as mineral polymorph type (Ruiz-Agudo and Putnis 2012). For example, several studies have shown that the presence of Mg^{2+} or Fe^{2+} in solution inhibits calcite growth (Astilleros et al. 2010; Di Lorenzo et al. 2017). This decrease in calcite growth rate can be explained based on a solid solution system, the incorporation of impurities in the crystal, its related change in the

✉ Yukun Ji
jykcumt@outlook.com

Veerle Vandeginste
veerle.vandeginste@kuleuven.be

Elliot Hocknull
ehocknull@mail.dstl.gov.uk

Hossein Fazeli
HosseinFazeli@iust.ac.ir

1 Department of Materials Engineering, KU Leuven, Campus Bruges, Bruges, Belgium

2 School of Chemistry, University of Nottingham, University Park, Nottingham NG7 2RD, UK

3 School of Chemical, Petroleum and Gas Engineering, Iran University of Science and Technology, Narmak, Tehran, Iran

4 State Key Laboratory for Geomechanics and Deep Underground Engineering, China University of Mining and Technology, Xuzhou 221116, Jiangsu, China

crystal surface structure, and a decrease in thermodynamic driving force for growth (Astilleros et al. 2010). The growth of a crystal is a complex process of several steps, with each step having an intrinsic activation energy (Di Lorenzo et al. 2017). The first step for the incorporation of a unit in the crystal structure involves the adsorption of cations onto the crystal surface, implying a coordinate bond formation with the crystal surface and alteration of the hydration shell. Then, the adsorbed cation continues to loose water molecules until its coordination is fully replaced by crystal units and the bonds obtain equilibrium values for the specific crystal structure. The adsorption of water molecules on dolomite differs with impurities in the crystals, with Fe weakening the adsorption capacity of water onto dolomite and Al enhancing it (Ao et al. 2022). Moreover, nucleation experiments of calcite in a solution containing also Fe^{2+} showed that the amount of Fe^{2+} has a key impact on the induction time and the maximum free calcium (Di Lorenzo et al. 2017).

Dolomitisation is one of the most important diagenetic processes in carbonate rocks, with significant implications for subsurface reservoirs and geological carbon dioxide storage. Notably, dolomite can store more carbon per unit volume, and it is more resistant to acidic corrosion, than calcite. Many earth scientists have been intrigued by the lack of abundant dolomite ($CaMg(CO_3)_2$) besides $CaCO_3$ in recent marine sedimentary systems, in contrast to ancient systems on Earth, despite the thermodynamic favourable conditions for dolomite formation (Warren 2000). Slow reaction kinetics impede dolomite formation (Sibley et al. 1987), and one of the most accepted causes is the strong hydration enthalpy of magnesium ions (Brady et al. 1996). In addition, low activity of dissolved carbonate relative to bicarbonate anions has been proposed as a factor that limits dolomite formation (Petrash et al. 2017). Still, given protodolomite, also called very high magnesium calcite, can readily form, additional kinetic factors linked to cation ordering in dolomite must also play a role (Meister et al. 2023). These kinetic factors could be linked to solid–liquid interfacial tension, surface charge and entropic effects, which may all be influenced by the solution composition and thus the specific ions in the solution.

Different background ions, and more specifically, their charge balance, through alkalinity, affect the fluid pH and carbonate speciation, and fluid pH impacts chemical reactions. Classical crystal growth theory links growth rate to degree of supersaturation. Still, the growth rate may also be affected via the Ph, since pH results in a change of the solution speciation, and thus the degree of supersaturation (Ruiz-Agudo and Putnis 2012), and a higher pH decreases the dolomite surface charge (Pokrovsky et al. 1999). In addition, the growth rate may be affected via the ionic strength of the solution, since background inorganic electrolytes can influence solubility due to strong long-range electric fields caused by the background ions reducing supersaturation and by the effect of cation hydration–dehydration dynamics governed by the strength of ion–water and ion–ion interactions, and thus entropic effects (Ruiz-Agudo and Putnis 2012), and a higher ionic strength amplifies the effect of pH on dolomite surface charge (Pokrovsky et al. 1999). Moreover, studies on surface energy and wettability of dolomite have indicated that interfacial tension can be reduced by oxalic acid-based and citric acid-based deep eutectic solvents, with the former outperforming the latter (Sanati et al. 2022). In addition, sulfate ions in water can alter the wettability of dolomite and enhance water adsorption (Safavi et al. 2020). An alkaline fluid pH has been conventionally suggested as being favourable for the formation of carbonate minerals, including dolomite (Arvidson and Mackenzie 1999; Warren 2000), since the carbonate ion is most abundant at alkaline conditions, whereas the bicarbonate ion and carbonic acid are most abundant at neutral and acidic conditions, respectively. Accordingly, naturally occurring carbonate has been explained by formation at alkaline pH conditions, for example, dolomite in sabkhas, playa lakes and hypersaline lagoons (Petrash et al. 2017), or environments with increased alkalinity driven by photosynthesis of cyanobacteria (Martinez et al. 2016). Dolomite is also found in environments with sulfate-reducing bacteria which consume organic acids (Braissant et al. 2007). However, sulfate reduction does not necessarily increase carbonate supersaturation, since it is coupled to H_2S oxidation with O_2 which produces acidity, as explained for calcium carbonate saturation in cyanobacterial mats (Aloisi 2008; Meister 2014). Some ephemeral lake environments (not linked to seawater) are highly alkaline and show ordered dolomite formation, as documented for e.g., the Deep Springs Lake and Lake Van, which is explained by fluctuations in conditions linked with microbially influenced processes (McCormack et al. 2018) and rate-limited growth model (Meister et al. 2011) related to favouring the stable phase (dolomite) by leaching the metastable phases (Deelman 1999). A similar interpretation was presented for microbial dolomite formation in Lake Neusiedl (Fussmann et al. 2020). Dolomite ripening under oscillating conditions, following Ostwald's step rule, was originally derived from experimental synthesis results (Deelman 1999; Liebermann 1967). Still, similar experiments with pH cycling led to the formation of magnesite in other studies (dos Anjos et al. 2011; Vandeginste 2021). In addition, the kinetic barrier that is specific to the formation of dolomite, thus the cation ordening, could be of entropic nature, and be related to the mineral surface, in particular the interfacial energy of a growing particle, which can be affected by oscillating environmental conditions (Meister et al. 2023). Furthermore, it has been suggested that alternating dolomite and chert beds may originate from pH changes related to CO_2 production by biogenic respiration in lake water and decomposition of

organic matter, resulting in pH decrease and dissolution of calcite and precipitation of silica (Kuma et al. 2019). Moreover, the complex nanoscale morphology of biomorphs, consisting of carbonate nanorods interwoven by amorphous silica, is controlled by local pH and supersaturation in an autocatalytic process (Garcia-Ruiz et al. 2009) in solution bulk pH of around 10 to 11 (Eiblmeier et al. 2013).

Alkaline, clay-rich soils have also been described as favourable environments for dolomite formation. Clay minerals are hydrous aluminium phyllosilicates, and thus aluminium is a key chemical element in clay environments. Moreover, previous research suggested that clay minerals may provide a source for magnesium to form dolomite (McHargue and Price 1982). However, more recent studies indicated that diagenetic Mg release from clay minerals cannot account for large scale dolomitisation, and that a seawater origin for magnesium is more likely (Li et al. 2016). The effect of aluminium on dolomitisation was not previously investigated, but there are several studies that show a favourable effect of clay on dolomite formation. Montmorillonite (a type of smectite) can be replaced by dolomite in soils of alkaline lakes (Casado et al. 2014). Dolomite is also often associated with sepiolite and palygorskite in alkaline lakes (Wanas and Sallam 2016; Wang et al. 2017). The presence of smectite clay also favours formation of dolomite in deeper soil levels in semi-arid regions, because water retained by the clay during evapotranspiration changes the local environment and transport properties, which enhance Mg incorporation in the calcite-to-dolomite replacement process (Diaz-Hernandez et al. 2013). Clay minerals have also been used as template for dolomite precipitation (Wanas and Sallam 2016), and negatively charged illite and smectite acted as catalysts and nucleation sites for dolomite formation (Liu et al. 2019). Similarly, a study on Eocene dolomite in evaporative lacustrine deposits suggests that clay surfaces present nucleation sites for the formation of dolomite at low temperature (Wen et al. 2020). Furthermore, a study on dolocrete in NW Australia indicated a close link between microbial extracellular polymeric substances (EPS) and mineralization of clay minerals and dolomite, with dolomite formation being promoted by the negatively charged surfaces of clay and EPS that help bonding and dehydration of Mg^{2+} and by the slow diffusion of ions through clay or EPS matrix (Mather et al. 2023). Despite the potential role of clay minerals in primary dolomite formation, there are relatively few studies on dolomite–clay mineral systems (Cai et al. 2021).

There are many examples of dolomite formation in alkaline environments, as shown above, and few studies that show dolomite formation in slightly acidic environments, even though several studies invoke pH cycling as a mechanism for dolomite formation, as mentioned above. Sulfide oxidation and resultant acid production was proposed as a mechanism for dolomite formation in the hypersaline coastal lagoon Brejo do Espinho (Moreira et al. 2004). In this process, the pore waters become undersaturated with respect to aragonite and high-Mg calcite, and supersaturated with respect to dolomite, and as they precipitate competitively (Arvidson and Mackenzie 1999), dolomite formation could be thermodynamically favoured (Moreira et al. 2004). Dolomitisation of the microbialites in the Ordovician Majiagou Formation in the Southern Ordos Basin is explained through formation by high-temperature acid fluids associated with the maturation of organic matter (Yang et al. 2022). Experiments with extreme halophilic bacteria suggest that dolomitisation of calcite is related to the presence of acidic amino acids and polysaccharides in the extracellular polymeric substances of the bacteria (Wang et al. 2022). However, in those experiments, dolomite formation is promoted with increasing carbonate alkalinity and pH, as carbonate anions can bind with Ca^{2+} and Mg^{2+} ions that are attracted to the negatively charged carboxyl groups of acidic amino acids and polysaccharides (Deng et al. 2010; Wang et al. 2022). Finally, our previous research has shown that zinc ions in saline fluids slightly decrease the fluid alkalinity to a pH of 6.7 and accelerate dolomitisation (Vandeginste et al. 2019). This leads to the following research question: *what is the impact of different background ions on the rate of dolomitisation?* Our goal with this work is to gain more clarity on the underlying mechanisms and factors, such as fluid acidity, ion hydration enthalpy, and chemical species distribution. Hence, this study is a step towards addressing the challenge of complexity and heterogeneity of natural systems.

In this work, we show that dolomitisation is faster in saline fluids that are slightly acidic due to the presence of ions with strong hydration enthalpies, in particular Lewis acids (electron pair acceptors). Based on the results of our experiments we identify and quantify the correlation between hydration enthalpy (amount of energy or heat released upon hydration) of the metal ions in solution and dolomitisation induction time. In addition, we present geochemical modelling that simulates the experimental conditions based on growth model and classical nucleation theory. The new insights suggest a different view for interpretations on the mechanisms, conditions and local environments that increase the rate of dolomitisation. We propose that dolomitisation can become faster in a saline, slightly acidic environment by the presence of background ions.

Materials and methods

Experimental design and materials

We hypothesize that background metal ions in solution can affect the rate of dolomitisation beyond the general

solution ionic strength effect (influencing dolomite dissolution kinetics (Xu et al. 2013)), and that the hydration enthalpy of the specific metal species correlates with the dolomitisation rate. To test this hypothesis, four types of batch reactor experiments were carried out in this study. Each experimental series followed the same overall procedure, but used different fluid compositions (Table 1). An aliquot of 200 mg calcite ($CaCO_3$) was added to 15 mL solution at room temperature in a Teflon-lined steel batch reactor (with volume of 25 mL), and the reactor was subsequently placed in a preheated oven at 200 °C. A series of reactors with the same fluid and powder was placed in the oven, as each sample measurement (reaction time step) is based on an individual reactor, that was removed from the oven at a given reaction time. This means that for one experimental series of a total of 24 h reaction time and 1 h interval, a total of 24 batch reactors was used. For triplicate measurements, this means 72 batch reactors. The pH was recorded at room temperature both in the starting fluid and in the fluid for each reaction time step upon cooling. The pH could be calculated by conversion from room temperature to 200 °C, and the predicted pH at 200 °C would be lower than that at room temperature. However, also the neutral pH value would be lower at 200 °C than at room temperature. Therefore, the pH is reported as it was measured at room temperature. A temperature of 200 °C and high salinity (2.00 mol L^{-1} NaCl or slightly less to obtain fluids of ionic strength of 3.5 in all experiments) were selected to enable comparison with a previous study in which the effect of dissolved zinc was tested (Vandeginste et al. 2019). Moreover, elevated temperature and fluid salinity are common in burial diagenetic settings, where dolomitisation can also take place. The amount of $CaCO_3$ and concentration of $MgCl_2$ and $CaCl_2$ in the fluids was kept the same for all experiments, and thus the dolomite saturation state was the same for the start of each experiment, to enable comparison between the different experiments and evaluation of the effect of background ions. All fluids contain 0.30 $MgCl_2$, 0.20 M $CaCl_2$, with Mg/Ca molar ratio of 1.5, shown to result in stoichiometric dolomite (Kaczmarek and Sibley 2011), and added NaCl up to 2 M, which accelerates the replacement reaction (Baker and Kastner 1981).

The first type of experiments (in triplicate with 1 h reaction time intervals) use the following solution composition: 0.30 mol L^{-1} $MgCl_2$, 0.20 mol L^{-1} $CaCl_2$, 1.55 mol L^{-1} NaCl and 0.03 mol L^{-1} $AlCl_3$. Addition of $AlCl_3$ in solution resulted in a decrease of the solution pH, leading to a fluid pH of 3.3. In the second type of experiments, the dissolved aluminium concentration was varied in seven duplicate experiments that were sampled after a time period of 8 h. Each of the solutions in those experiments contain 0.30 mol L^{-1} $MgCl_2$ and 0.20 mol L^{-1} $CaCl_2$, but the $AlCl_3$ concentration was varied, and NaCl concentration as well to maintain the solution ionic strength of 3.5, resulting in the following concentrations: (1) 2.00 mol L^{-1} NaCl, (2) 1.85 mol L^{-1} NaCl and 0.01 mol L^{-1} $AlCl_3$, (3) 1.70 mol L^{-1} NaCl and 0.02 mol L^{-1} $AlCl_3$, (4) 1.32 mol L^{-1} NaCl and 0.045 mol L^{-1} $AlCl_3$, (5) 1.10 mol L^{-1} NaCl and 0.06 mol L^{-1} $AlCl_3$, (6) 0.80 mol L^{-1} NaCl and 0.08 mol L^{-1} $AlCl_3$, (7) 0.50 mol L^{-1} NaCl and 0.10 mol L^{-1} $AlCl_3$. The third type of experiments (in triplicate with 1 h reaction time intervals) tests the effect of solution pH. In this case, no $AlCl_3$ was added to the solution, but the solution pH was decreased to 3.3 (as measured in the first type of experiments) by addition of trace element grade HCl. The experimental series uses a solution composition of 0.30 mol L^{-1} $MgCl_2$, 0.20 mol L^{-1} $CaCl_2$, 2.00 mol L^{-1} NaCl, and minor amount of HCl to reach pH of 3.3. Finally, the fourth type of experiments has a solution composition of 0.30 mol L^{-1} $MgCl_2$, 0.20 mol L^{-1} $CaCl_2$, 1.97 mol L^{-1} NaCl and 0.03 mol L^{-1} KCl. The starting pH of this solution is 9.3.

All solutions were prepared with milliQ water. $CaCO_3$ was purchased from Acros Organics, NaCl and KCl from

Table 1 Overview of fluid starting compositions of all experiments. Concentrations are presented in mol L^{-1}

Experiment	NaCl	$MgCl_2$	$CaCl_2$	$ZnCl_2$	$AlCl_3$	KCl	HCl	pH start
Control	2.00	0.30	0.20	0	0	0	0	8.6
$ZnCl_2$	1.91	0.30	0.20	0.03	0	0	0	6.7
$AlCl_3$ (0.01)	1.85	0.30	0.20	0	0.01	0	0	3.6
$AlCl_3$ (0.02)	1.70	0.30	0.20	0	0.02	0	0	3.3
$AlCl_3$ (0.03)	1.55	0.30	0.20	0	0.03	0	0	3.3
$AlCl_3$ (0.045)	1.32	0.30	0.20	0	0.045	0	0	3.1
$AlCl_3$ (0.06)	1.10	0.30	0.20	0	0.06	0	0	3.0
$AlCl_3$ (0.08)	0.80	0.30	0.20	0	0.08	0	0	2.9
$AlCl_3$ (0.10)	0.50	0.30	0.20	0	0.10	0	0	2.9
KCl	1.97	0.30	0.20	0	0	0.03	0	9.3
HCl	2.00	0.30	0.20	0	0	0	0.0005	3.3

The pH values are those measured at room temperature

VWR Chemicals, HCl from Fisher Chemicals, $AlCl_3.6H_2O$ from APC Pure, $CaCl_2$ from Merck, and $MgCl_2$ from Alfa Aesar.

Analytical methods

The reaction solids (referring to all solid material present in the reactor at the time of sampling) from each batch reactor were collected by centrifugation and three rinsing steps with milliQ water and centrifugation at high speed to remove any potential NaCl salt from the reaction products. Upon decanting the liquid, the reaction products were then dried in an oven at 50 °C for 3 days. After complete drying, the weight of the reaction products was recorded. The composition of the reaction solids assemblage was analysed by powder X-ray diffraction (XRD), using a PANalytical X'Pert Pro X-ray diffractometer with CuKα radiation at a tube voltage of 40 kV and current of 40 mA. The reaction solids were scanned over a sampling range of 5 to 70 ° 2θ, with a step size of 0.0066° and a scan speed of 0.023 ° 2θ per second. Data were analysed for phase identification by comparison with reference spectra within the PDF4 database from the International Centre for Diffraction Data. Identification and quantification of the different minerals in the reaction products was completed using Profex software with Rietveld analysis. In the results below, "(proto)dolomite" indicates the combined amount of protodolomite (or also called very high magnesium calcite) and dolomite, which have the same main peaks, such as the 104 diffraction peak. The main differences in the diffractograms of dolomite and protodolomite is the lack of the ordering peaks (such as 015 diffraction peak) in protodolomite. The reaction solids were also analysed by Fourier Transform Infrared (FTIR) spectrometry using a Bruker Alpha FTIR spectrometer with OPUS software to record transmittance for the wavenumber range of 400–4000 cm^{-1}. Imaging of the reaction solids has been conducted using a JEOL JSM-7100F Field Emission Gun Scanning Electron Microscope. The Brunauer–Emmett–Teller (BET) surface area of the calcite powder used in the batch reactor experiments was determined by triplicate analysis (on samples of more than 1 g) using a Micromeritics 3Flex instrument with nitrogen gas for surface characterization, and has a value of 8.72 ± 0.04 m^2/g.

Modelling

In this study, calcite and dolomite are the only minerals considered and their reaction rates are computed kinetically. Dissolution is modelled following the TST approach (Aagaard and Helgeson 1982):

$$r_+ = k_+ S \prod_i^n a_i^{\nu+} \exp\left(-\frac{\mathrm{Ea}_+}{RT}\right)\left(1 - \frac{\Delta G_\mathrm{R}}{RT}\right), \tag{1}$$

and precipitation is modelled using the combination of a simplified second-order BCF (Burton Cabrera and Frank) growth model (Burton et al. 1951) and classical nucleation theory (Pham et al. 2011):

$$r_- = k_- S \prod_i^n a_i^{\nu-} \exp\left(-\frac{\mathrm{Ea}_-}{RT}\right)(\Omega - 1)^2 - k_N \exp\left(-\Gamma\left(\frac{1}{(T)^{2/3}\ln\Omega}\right)^2\right), \tag{2}$$

where r is reaction rate (mol/s), k is the reaction rate coefficient (mol/m^2 s), S is the reactive surface area (m^2), a is the activity of species i in the aqueous solution, ν is the reaction order, Ea is the apparent activation energy, R is the gas constant, T is the absolute temperature, ΔG_R is the free energy of the reaction, Ω is saturation ratio, k_N is the nucleation rate constant, Π is a product operator, and Γ is a constant, where it represents the effects of surface tension, molar volume, and the geometric surface shape factor (Pham et al. 2011). The plus and minus subscripts show the dissolution and precipitation reactions, respectively. In the above equations, the reactive surface area is calculated by.

$$S = \beta M n, \tag{3}$$

where n is the number of moles of the mineral, M is molar weight, and β is the specific surface area. PHREEQC v3 (Parkhurst 1995) was used to perform the geochemical modelling. The llnl.dat thermodynamic database included with the PHREEQC v3 (Parkhurst 1995), was used for the aqueous speciation and for minerals. The parameters used for Eqs. (1–3) are summarized in Table 2.

The initial fluid compositions used in PHREEQC modelling are listed in Table 1, and the initial calcite in the

Table 2 Parameters used for equations in geochemical modeling of this study

Mineral	k_+ (mol/m^2 s)	Ea_+ (kJ/mol)	$k\_$ [a] (mol/m^2 s)	Ea_ (kJ/mol)	Γ	S (m^2/g)
Calcite	$10^{-0.3}$ (Palandri and Kharaka 2004)	14.4 (Palandri and Kharaka 2004)	–	–	–	8.72
Dolomite	–	–	4.5×10^{-25} (Arvidson and Mackenzie 1999)	133.5 (Arvidson and Mackenzie 1999)	2.35×10^{10}	0.016 (Pokrovsky et al. 2005)

[a] $k\_$ is reaction rate coefficient at 25 °C and pH 5

simulations was 200 mg in 15 ml solution. The temperature in the simulation was 200 °C.

Results

Dolomitisation reaction and byproduct formation

The experimental results show that the addition of 0.03 mol L^{-1} $AlCl_3$ to the NaCl–$MgCl_2$–$CaCl_2$ solution causes a low starting pH of 3.3 ± 0.1 due to the hydrolysis of Lewis acid $AlCl_3$ in water. This leads to dissolution of about 20% of the calcite reactant within the first hour based on reaction solids weight of 157 ± 4 mg. Reaction products are detected after 3 h (Fig. 1) based on XRD (Fig. 2a) and FTIR analyses (Fig. 3a). The reaction does not only result in the formation of (proto)dolomite, but up to 30% of the reaction solids is hydrotalcite (Figs. 2a, 4a) with its highest content measured at 8 h reaction time (Fig. 1). Hydrotalcite is a layered double hydroxide, and occurs as a rare natural mineral on Earth (Tao et al. 2019). Hydrotalcite consists of positively charged brucite-like oxide layers [$Mg_3Al(OH)_8$], charge-balancing interlayer carbonate anions, and interlayer water (Ishihara et al. 2013). In addition, a minor amount of pseudoboehmite [AlO(OH)], a synthetic pure pseudocrystalline aluminium hydroxide gel (Calvet et al. 1952), is identified based on the XRD patterns of the reaction solids (Figs. 1, 2a), which are similar to that of well-crystallized boehmite but with broadening and different relative intensities of the peaks (Santos et al. 2009; Yang et al. 2012).

The experiments with differing Al concentrations (up to 0.10 mol L^{-1} $AlCl_3$) in saline fluids indicate that the Al concentration has a significant impact on the fluid starting pH and on the time-dependent reaction solids composition

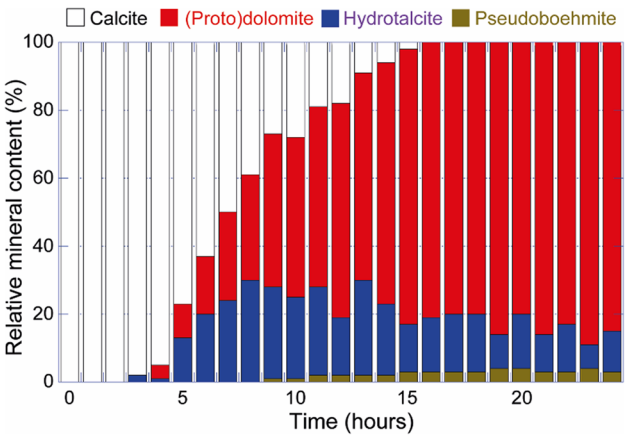

Fig. 1 Reaction solids calcite, (proto)dolomite, hydrotalcite and pseudoboehmite mineral cumulative percentages as a function of reaction time in the 0.03 mol L^{-1} $AlCl_3$ experiment

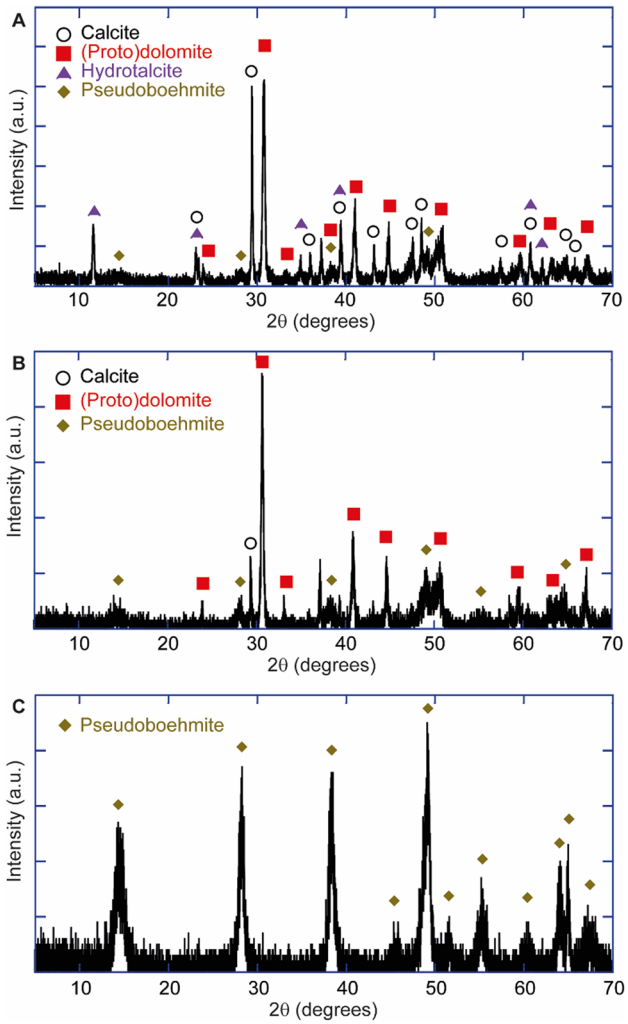

Fig. 2 Powder X-ray diffractograms of reaction products in **a** the 0.03 mol L^{-1} $AlCl_3$ experiment at 10 h reaction time, **b** the 0.045 mol L^{-1} $AlCl_3$ at 8 h reaction time and **c** the 0.10 mol L^{-1} $AlCl_3$ at 8 h reaction time

(Fig. 5). For a reaction time of 8 h, the weight of the reaction solids decreases roughly linearly from 191 to 117 mg with increasing Al concentration of up to 0.08 mol L^{-1} $AlCl_3$, and then a larger decrease down to 29 mg for the 0.10 mol L^{-1} $AlCl_3$ experiment (Fig. 5a). The experiments with up to 0.06 mol L^{-1} $AlCl_3$ have a pH of 5.2–5.5, the 0.08 mol L^{-1} $AlCl_3$ experiment a pH of 4.6, and the 0.10 mol L^{-1} $AlCl_3$ experiment a pH of 1.5 (Fig. 5b). The 0.045 mol L^{-1} $AlCl_3$ experiment (at 8 h reaction time) has the highest relative percentage of (proto)dolomite with only minor contents of calcite and pseudoboehmite, and lack of hydrotalcite (Figs. 2b, 5c). The reaction solid of the 0.10 mol L^{-1} $AlCl_3$ experiment consists entirely of pseudoboehmite (Fig. 4b) based on XRD (Fig. 2c) and FTIR spectra with disappearance of the asymmetric stretching of CO_3 band at 1390–1510 cm^{-1} (Fig. 3b).

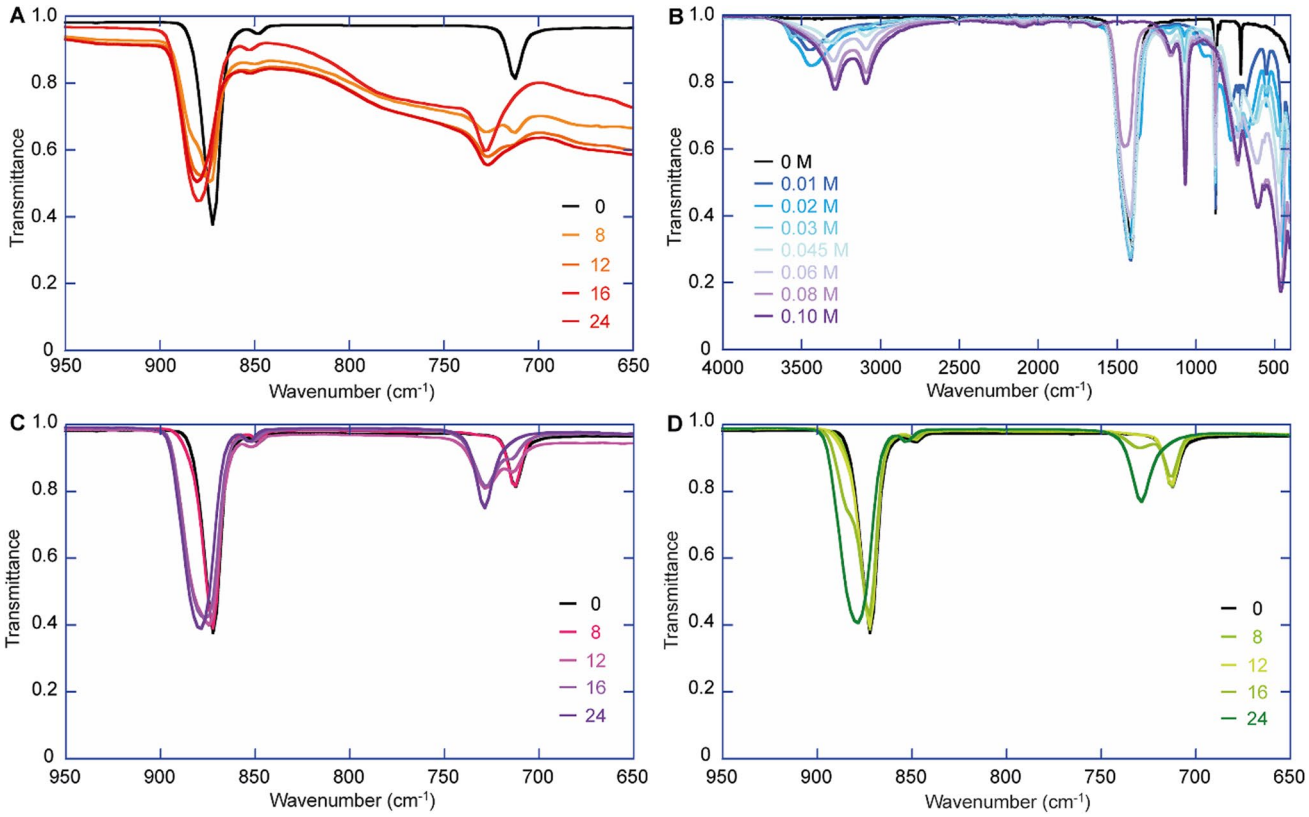

Fig. 3 FTIR spectra of the reaction products in **a** the 0.03 mol L^{-1} $AlCl_3$ experiment at the labelled reaction times in hours, **b** the experiments with the labelled aluminium concentrations for 8 h reaction time, **c** the HCl experiment with starting fluid pH of 3.3 at the labelled reaction time in hours, and **d** the 0.03 mol L^{-1} KCl experiment at the labelled reaction times in hours. Note the selected 650–950 cm^{-1} interval in **a**, **c** and **d** in contrast to the full 400–4000 cm^{-1} in **b**

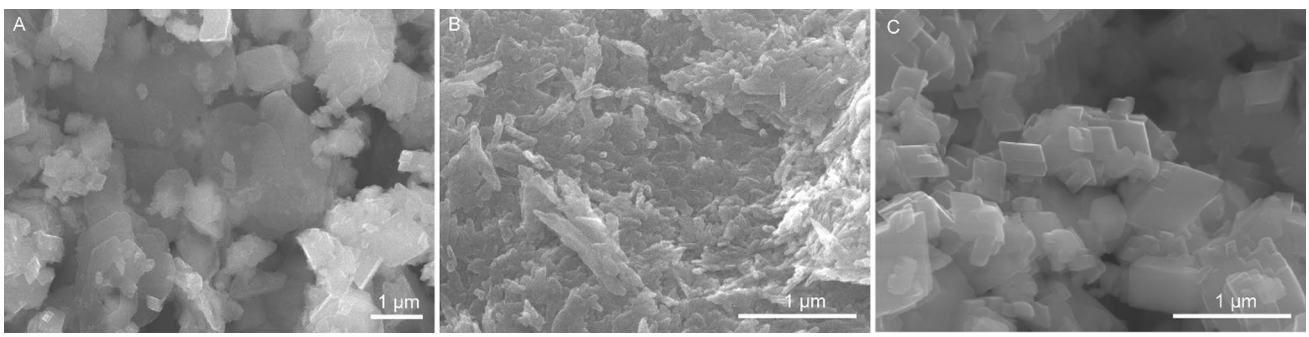

Fig. 4 Scanning electron microscope images of reaction solid from **a** 0.03 mol L^{-1} $AlCl_3$ experiment at 24 h reaction time, with rhombohedral dolomite crystals and hexagonal shaped platelets of hydrotalcite, **b** 0.10 mol L^{-1} $AlCl_3$ experiment at 8 h reaction time with pseudoboehmite, and **c** HCl pH 3.3 experiment with rhombohedral dolomite crystals

In the experiments with HCl and those with KCl, no byproducts were detected based on SEM (Fig. 4c), XRD and FTIR (Fig. 3c, d). The HCl experiments have a starting fluid pH of 3.3, and the pH increases to 5.7 ± 0.3 within 1 h, without much dissolution of calcite, based on the reaction solids weight of 197 mg. A much higher starting fluid pH (9.3) is measured in the experiments with 0.03 KCl, and no calcite dissolution phase precedes the interface-coupled dissolution–precipitation of the dolomitisation process.

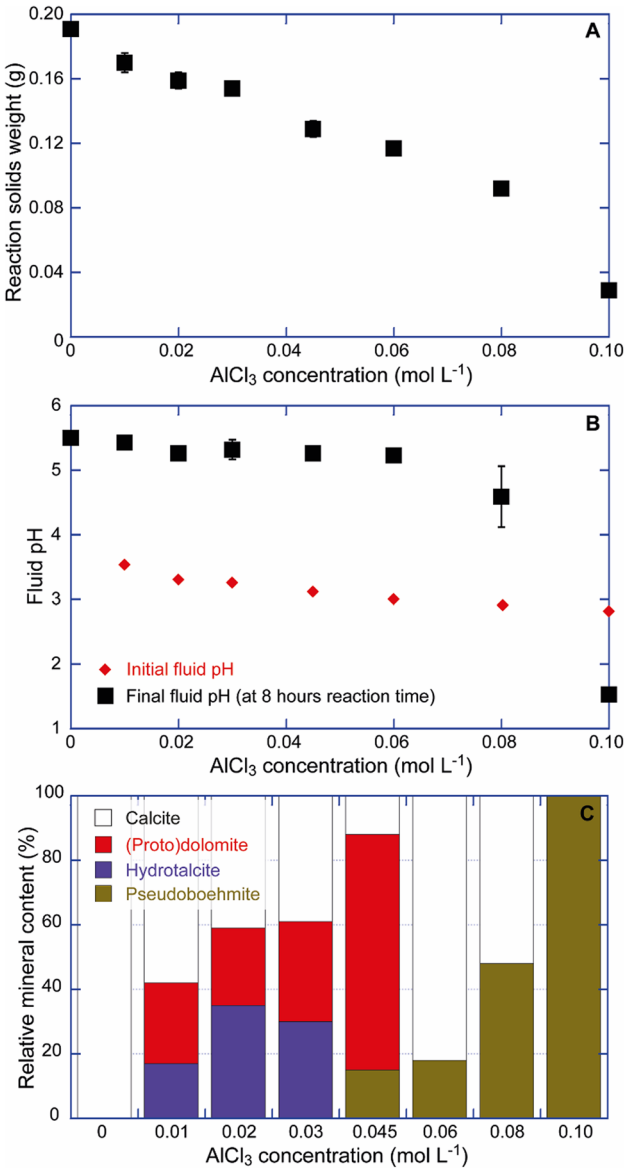

Fig. 5 Experimental data at 8 h reaction time for dolomitisation with fluids of differing aluminium concentrations. **a** Reaction solids weight decreases with increasing $AlCl_3$ concentration. **b** Final fluid pH is similar for $AlCl_3$ concentration up to 0.06 mol L^{-1} and decreases significantly with even higher $AlCl_3$ concentration. **c** Relative content of calcite, (proto)dolomite, hydrotalcite and pseudoboehmite in the reaction solids changes with different $AlCl_3$ concentrations in the fluids

Dolomitisation rate

The 0.03 mol L^{-1} $AlCl_3$ experiment shows a dramatic decrease in induction time, from 10.5 to 3.5 h, and in timing of full conversion from calcite to (proto)dolomite, from 23 to 16 h, in comparison with control experiments (Fig. 6a). The (proto)dolomite and hydrotalcite content in the reaction solids increases between 4 and 8 h reaction time, after which the (proto)dolomite content keeps increasing, in contrast to the hydrotalcite content which shows a general slight decrease after 8 h reaction time (Fig. 1). The dolomitisation rate increases with aluminium concentration up to 0.045 mol L^{-1} $AlCl_3$ (Fig. 5c). However, the experiments with concentrations of 0.06 to 0.10 mol L^{-1} $AlCl_3$ lead to the formation of pseudoboehmite (Figs. 2c, 3, 4b, 5c).

The HCl (pH 3.3) experiments show an induction time of 6.5 h and full conversion time of 18 h (Fig. 6a) based on XRD and FTIR analysis (Fig. 3c) with the bands at 714 and 728 cm^{-1} being assigned to ν_4 in-plane bending of CO_3 in calcite and dolomite, respectively (Wang et al. 2019). The 0.03 mol L^{-1} KCl experiments indicate an induction time of 13.5 h, which is longer than that of the control experiments (10.5), and a full conversion time of 24 h (Fig. 6a) based on XRD measurements and FTIR spectra (Fig. 3d). The dolomitisation reaction rates are fitted using the Avrami equation, with reaction extent $y = 1 - \exp[-(k(t - t_0))^n]$ whereby t_0 is the induction time, k the rate constant and n the time exponent (Fig. 6b). The Avrami equation simulates the transformation from one phase to another at constant temperature and has been used for fitting the rate of dolomitisation in some previous studies (Rodriguez-Blanco et al. 2015; Xia et al. 2009). The derived reaction rate constants from our results increase in the order of HCl < control (NaCl) < $AlCl_3$ < KCl < ZnO < $ZnCl_2$ experiments, indicating the lack of overall correlation between decreasing induction time ($AlCl_3$ < $ZnCl_2$ = ZnO < HCl < control (NaCl) < KCl) and increasing Avrami rate constant (Table 3).

Discussion

The presence of background compounds in solution influences the starting pH of the solution, which in turn can influence calcite dissolution and dolomite precipitation. Even though the ionic strength (which affects the activity of species in solution) is kept the same in all solutions, the measurements show that the fluid starting pH is still influenced by the different interaction of ion assemblages with water in the experiments. At alkaline conditions, the carbon speciation increases in the order of $CO_2 < HCO_3^- < CO_3^{2-}$, resulting in a high carbonate mineral saturation index, favourable for carbonate formation. According to classical crystal growth theory, the growth rate is related to degree of supersaturation. However, the presence of background ions may induce non-classical crystallization pathways. For example, calcite nucleation and growth rate decrease with increasing alkaline pH from 7.5 to 12 in supersaturated solutions of low ionic strength of 0.1, due to strongly hydrated hydroxyl ions that lead to increased frequency of water exchange with hydrated

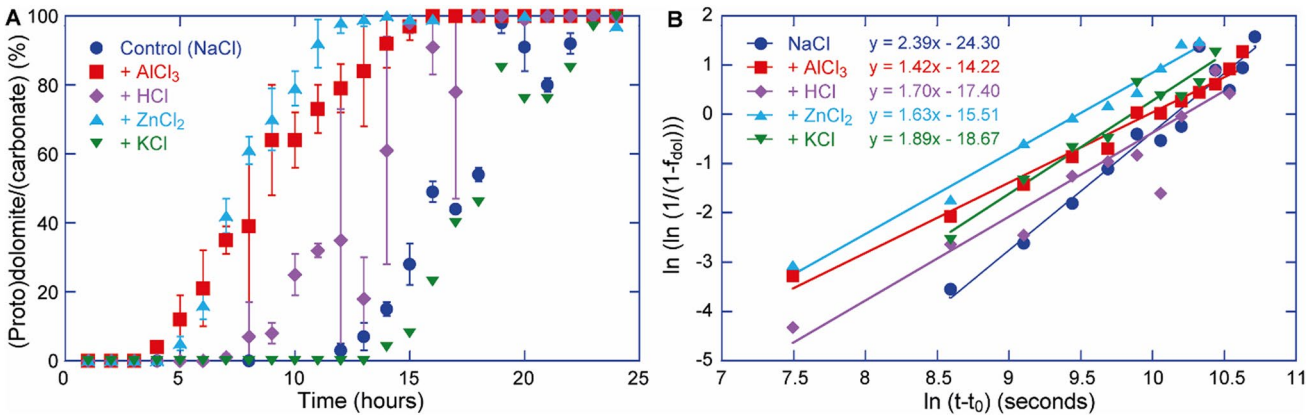

Fig. 6 **a** Calcite-to-dolomite replacement reaction curves presenting (proto)dolomite on total carbonate percentage against reaction time. The plot presents experimental data from this study for the 0.03 mol L^{-1} $AlCl_3$, 0.03 mol L^{-1} KCl and HCl added to reach pH 3.3, whereas the control experiment and 0.03 mol L^{-1} $ZnCl_2$ experimental data are from our previous work (Vandeginste et al. 2019). **b** Avrami plot for dolomitisation in the different experiments with linear best fit trend lines to derive time exponent and rate constant

Table 3 Best fit parameters for the Avrami model of the dolomitisation rates in the different experiments with t_0 the induction time, k the rate constant and n the time exponent for the Avrami equation with reaction extent $y = 1 - \exp[-(k(t - t_0))^n]$

Experiment	t_0	k (s^{-1})	n
Control	10.5	3.9×10^{-5}	2.4
$ZnCl_2$	4.5	7.6×10^{-5}	1.6
ZnO	4.5	7.2×10^{-5}	1.8
$AlCl_3$	3.5	4.6×10^{-5}	1.4
HCl	6.5	3.6×10^{-5}	1.7
KCl	13.5	5.2×10^{-5}	1.9

The data for the control and Zn experiments are from Vandeginste et al. (2019)

calcium ions, causing increased solid–liquid interfacial tension and reducing the nucleation rate (Ruiz-Agudo et al. 2011a). The alternating Ca^{2+} and CO_3^{2-} ions in calcite generate a polar hydrophilic surface, with which the hydroxyl group of water strongly interacts through electrostatic interaction (between O from hydroxyl and Ca from the calcite surface) and by hydrogen bonding (between H from hydroxyl and O from the calcite surface) (Hakim et al. 2017). These studies show that faster carbonate nucleation and growth is not always linked to higher alkalinity due to interfacial tension effects. The carbon speciation in our experiments was reconstructed through PHREEEQC modelling, and shows a decrease in the order $CO_2 > HCO_3^- > > CO_3^{2-}$ in the 0.03 mol L^{-1} $AlCl_3$ and HCl experiments with starting fluid pH of 3.3, and $HCO_3^- > CO_2 > > CO_3^{2-}$ in the 0.03 mol L^{-1} $ZnCl_2$ experiments with starting pH of 6.7 (Fig. 7). The control and 0.03 mol L^{-1} KCl experiments with starting pH of 8.5 and 9.3, respectively, have a carbon speciation with $HCO_3^- > CO_3^{2-} > CO_2$ (Fig. 7). The modelled pH at the end of the simulation is 4.9, 5.8, 6.9, 8.5 and 9.3 for the 0.03 mol L^{-1} $AlCl_3$, HCl, 0.03 mol L^{-1} $ZnCl_2$, control and 0.03 mol L^{-1} KCl experiments, respectively. Hence, these PHREEQC results based on classical nucleation theory and growth model indicate that CO_3^{2-} ions are not the dominant carbon species. Notably, the carbon species absolute values show that the CO_3^{2-} activity in the $ZnCl_2$ experiment (with the fastest complete conversion of calcite to dolomite) is less than half that in the other experiments. Still, we need to consider that the CO_3^{2-} activity could remain low during the dolomitisation process, where released carbonate ions from calcite dissolution could immediately be incorporated in the precipitating dolomite.

Our laboratory experiments indicate faster dolomitisation in slightly acidic fluids. The fluid pH decreases in solutions with cations that have a strong hydration enthalpy (i.e., energy or heat released upon hydration of the cations). Acidic fluids can cause faster calcite dissolution, which then leads to a faster increase in calcium and carbonate ions in solution; and the pH was less than 6 at 1 h reaction time in all experiments. Considering a first order reaction rate for the precipitation of dolomite, a faster increase of carbonate ion concentration in solution could explain a faster dolomitisation rate, and PHREEQC modelling results support faster dolomitisation in slightly acidic than in alkaline fluids (Fig. 8). This could be interpreted based on the thermodynamic drive that the solution is undersaturated with respect to calcite and oversaturated with respect to dolomite when Ca^{2+} comes into solution upon calcite dissolution.

Furthermore, we compared the effect of $AlCl_3$ versus HCl in solution at the same pH of 3.3. The experimental results demonstrate that the dolomitisation induction time does not only depend on the fluid pH but also on the ion assemblage, with Lewis acid $AlCl_3$ being more effective

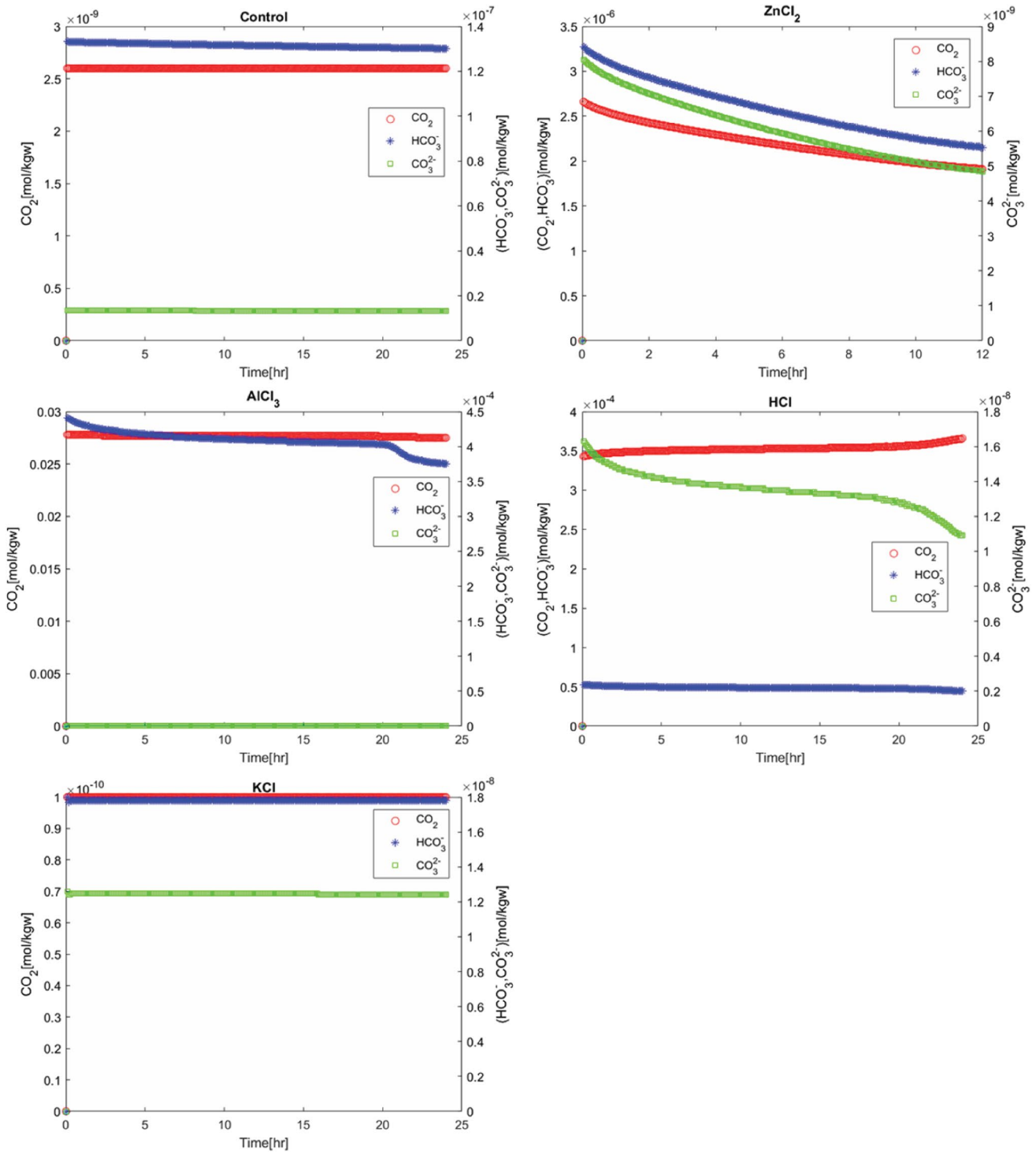

Fig. 7 Plots of the PHREEQC modelled carbon species distribution against time, simulating the control and $ZnCl_2$ experiments (Vandeginste et al. 2019), and the 0.03 mol L^{-1} $AlCl_3$, HCl and KCl experiments presented in this study

in shortening the dolomitisation induction time than Brønsted acid HCl (Fig. 9). The PHREEQC modelling results do not completely align here with the experimental data (Fig. 8), and also the shorter induction time for the $AlCl_3$ experiment in comparison with the $ZnCl_2$ experiment is not evident in the models. Given that hydrotalcite and some pseudoboehmite form besides dolomite in the 0.03 mol L^{-1} $AlCl_3$ experiments, the dolomitisation rate

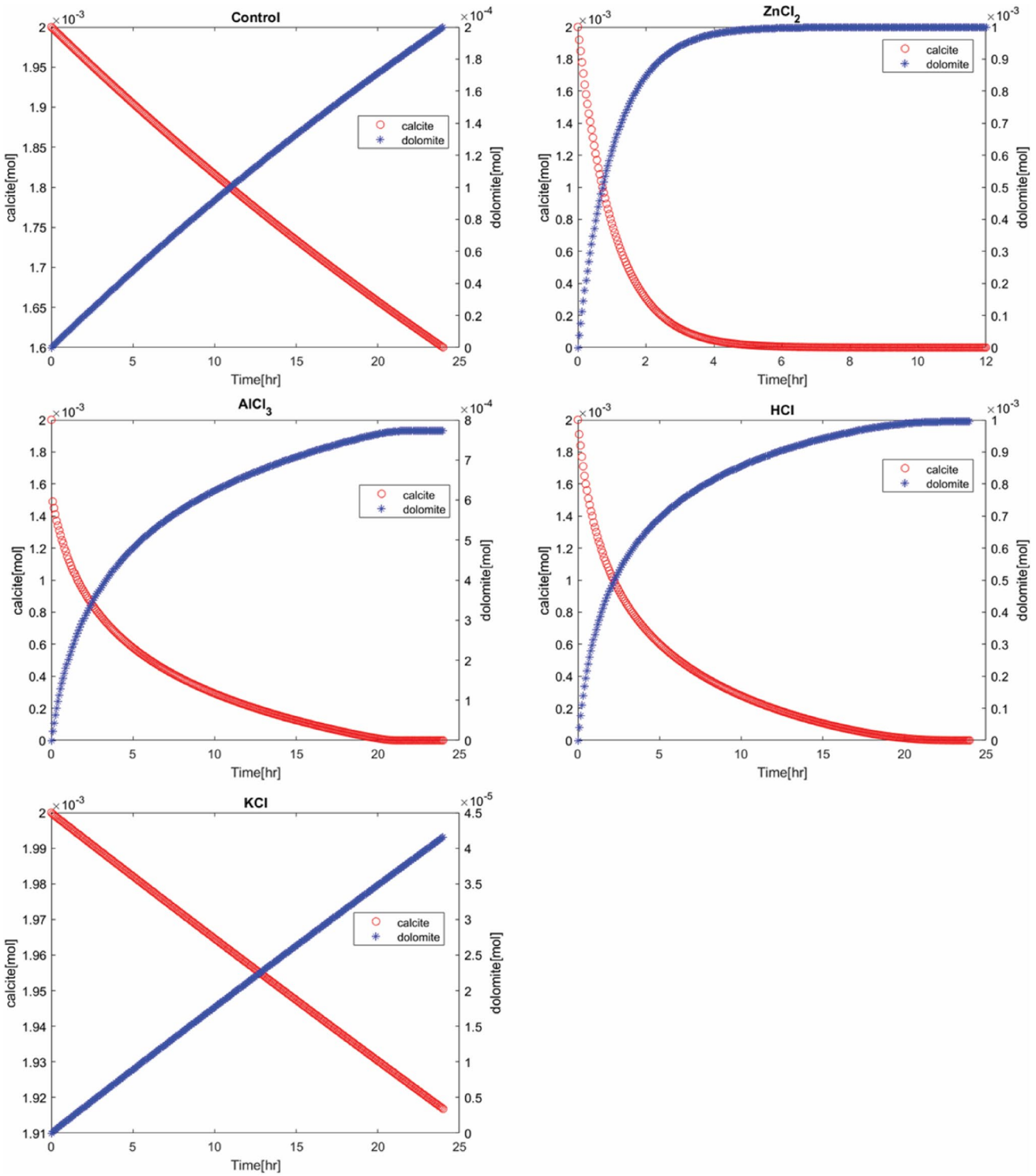

Fig. 8 Plots of the PHREEQC modelled number of moles calcite and dolomite against time, simulating the control and $ZnCl_2$ experiments (Vandeginste et al. 2019), and 0.03 mol L^{-1} $AlCl_3$, HCl and KCl experiments described in this study

may be more complicated in this case. The general trends in the experimental dolomitisation work are consistent with the PHREEQC results, and given these results are based on classical crystallization theory, we think that the slight discrepancies between the laboratory experimental data and the PHREEQC results are probably caused by specific ion effects, inducing non-classical crystallization pathways.

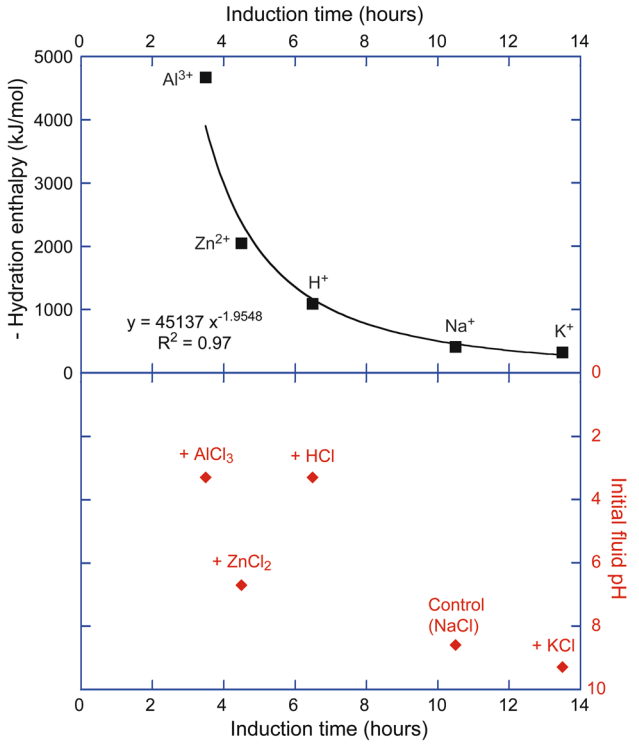

Fig. 9 Plots of the relation between dolomitisation induction time (based on experimental results in this study) with the positive hydration enthalpy values of the cation added to the solution (black squares) and the initial fluid pH (based on the experimental data in this study; red diamonds). The hydration enthalpy of Na^+ is used for the control experiment, since the amount of NaCl in solution is decreased in the other experiments for addition of other salts to maintain equal solution ionic strength in all experiments. A power law trend line equation is derived for positive hydration enthalpy values against dolomitisation induction time

The effect of specific ions in solution at mineral or other material surfaces are determined by a balance between different forces that are influenced by the characteristics of the ion, the solvent and the surface properties (Moghaddam and Thormann 2019). Therefore, solution composition, mineral surface, surface charge, interfacial tension and entropic effects are all important factors that may influence crystal nucleation and growth rate. Hydration of ions plays thereby a major role, with competition between ion–water (electrostatic) and water–water (hydration) interactions, and also the material surface properties. For example, dolomite growth can be accelerated with carboxylated polystyrene spheres due to the favourable impact of the surface carboxyl functional groups on complexation and dehydration of magnesium ions (Roberts et al. 2013). The results of our study, showing a shorter dolomitisation induction time in fluids with stronger cation hydration enthalpy, are different to the impact of background ions on calcium carbonate nucleation in dilute solutions, where the induction time decreases with increasing ionic radii of background ions (Burgos-Cara et al. 2017), generally correlating with weaker hydration enthalpy. In dilute solutions, an entropic effect related to changes in ordering of water molecules due to arrangement as hydration shells around ions (that build up the mineral) plays a dominant role (Ruiz-Agudo et al. 2011b). In fluids of high ionic strength, there are more interactions between the background ions and water molecules, and thus the competition for hydration water is higher (Ji et al. 2022), and ion hydration becomes the dominant factor controlling kinetics (Ruiz-Agudo et al. 2011b). A study on the effect of background ions on the rate of dolomite dissolution reported a higher dolomite dissolution rate in saline solutions (with ionic strength of 1) with NaCl in comparison with KCl (Ruiz-Agudo et al. 2011b). Since Na^+ has a stronger hydration enthalpy and smaller ionic radius than K^+, these results imply a faster dolomite dissolution rate in fluids with background ions that have a stronger hydration enthalpy. In solutions of high ionic strength, the relative impact of background ions on the dolomite dissolution rate is determined by water–water interactions and effects associated with the strong hydration of calcium and magnesium ions (Ruiz-Agudo et al. 2011b). The K^+ ion weakens the structure of water (due to higher ion mobility), and competition for hydration water between the bulk and the solute ions is lower in a less structured solvent, and therefore, the water exchange frequency will be lower, resulting in slower dolomite dissolution (Ruiz-Agudo et al. 2011b). Our study concerns dolomite formation rather than dolomite dissolution, and still, our results show a similar effect, namely, faster dolomitisation in saline fluids (with even higher ionic strength) with background ions that have a stronger hydration enthalpy. Magnesium ion dehydration and incorporation in the dolomite crystal during dolomitisation is thus more favourable in water composed of background ions with a stronger hydration enthalpy, and thus more structured water. This is interpreted by the fact that removal of magnesium ions from the water may have a small entropic effect on the structured water, and that competition for hydration water is very high in these highly saline fluids, so that that ions with stronger hydration enthalpy in the water would compete for hydration water, and in this way, favour magnesium ion dehydration.

In contrast to induction time, the Avrami derived rate constant for dolomitisation in the different solutions seems to be not only affected by the hydration enthalpy but also by the complexity of the fluid composition and the formation of byproducts in the dolomitisation reaction. Our experiments focused on the effect of positively charged background ions in solution. Negatively charged background ions can also accelerate mineral growth by enhanced ion dehydration.

However, this may be counteracted by ion pair formation which lowers mineral supersaturation, as documented, for example, by the inhibiting effect of sulfate on the formation of magnesite (King et al. 2013) and dolomite (Baker and Kastner 1981; Vandeginste et al. 2019).

The rate of geochemical reactions is commonly derived from laboratory experiments, where the experimental conditions are simplified to derive fundamental correlations based on one or a few variable parameters. These laboratory-derived rates then serve as data and input for models that simulate real natural scenarios. However, the combined effect of several parameters together could lead to different results than the simple combination of the effects of the parameters tested separately, for example, by the specific ion effect linked to the presence of background ions. As a consequence, interpretations on natural environments or prediction for geological carbon storage could then be inaccurate. Several studies have highlighted the complexity of natural systems and associated challenges in interpretations. There are discussions around the influence of associated minerals on dissolution processes in carbonate rocks, since additional metal ions, such as Fe^{3+}, in acidic fluids, have shown to change the fluid properties and dissolution behaviour (Ma et al. 2021). A study reports the role of the fluid environment (pH and composition) in determining the surface charge of the interface of minerals and brine, with implications for wettability in reservoirs (Mohammed et al. 2022). Different minerals behave differently in an environment of varying composition and salinity (Mohammed et al. 2022). Fluid inclusion studies have documented thermal and chemical fluid heterogeneity, which is common in large paleohydrothermal systems with recharge of surface-derived fluids (Wilkinson 2010). Understanding and reconstructing the geological history of mineralization is important in ore field studies, for example, Zn–Pb deposits in dolomitized host rocks (Wilkinson 2010). Studies on smart waters for enhanced oil recovery in carbonate reservoirs report that the complexity of the fluids/rock system governs the effects and that the fundamental knowledge is still lacking, and thus many questions and uncertainties remain (Gachuz-Muro et al. 2017). The challenge of complexity of natural systems and resulting inaccurate predictions could be overcome by taking measurements in the field or using the actual formation fluids in laboratory experiments. Still, this offers only a solution case by case, and not a global approach. A more fundamental approach that documents the effect of background ions could help in achieving more realistic predictions for natural scenarios. Previous experiments demonstrate the need to incorporate the specific ion effect in predictive models that simulate mineral formation and dissolution in natural complex systems (Ruiz-Agudo et al. 2011b). Our study contributes in unravelling the effect of some background ions on the rate of dolomitisation.

Conclusion

We have documented that the dolomitisation induction time decreases with stronger hydration enthalpy of background ions in saline solutions of the same ionic strength. This observation is mainly caused by the slightly acidic pH, and by the specific ion effect. These results highlight the importance of fluid complexity or heterogeneity with implications for interpretations of natural environments or predictions for geological carbon storage.

Acknowledgements The authors thank the Nanoscale and Microscale Research Centre, the School of Chemistry and the GeoEnergy Research Centre for providing access to instrumentation at the University of Nottingham. We thank Elisabeth Steer for help with SEM analyses, Stephen Argent, Mark Guyler and Martin Roe for help with instruments, and Andrei Khlobystov for valuable discussions. This work was partly funded by KU Leuven Internal Funds Bijzonder Onderzoeksfonds 2020 (Grant number STG/20/013), the Natural Science Foundation of Jiangsu Province (BK20221135), and the National Natural Science Foundation of China (42307202).

Author contributions VV conceptualization, methodology, validation, investigation, writing—original draft and review and editing, visualization, supervision; EH investigation, validation; HF software, investigation, formal analysis, visualization; YJ investigation, writing—review and editing

Data availability Data presented in this paper can be made available upon request to the authors.

Declarations

Conflict of interest The authors declare no competing interests.

References

Aagaard P, Helgeson HC (1982) Thermodynamic and kinetic constraints on reaction-rates among minerals and aqueous-solutions. 1. Theoretical considerations. Am J Sci 282:237–285. https://doi.org/10.2475/ajs.282.3.237

Aloisi G (2008) The calcium carbonate saturation state in cyanobacterial mats throughout Earth's history. Geochim Cosmochim Ac 72:6037–6060. https://doi.org/10.1016/j.gca.2008.10.007

Ao XQ, Chen H, Yang C, Li CQ, Jiang CY (2022) A first-principle study of the effect of Fe/Al impurity defects on the surface wettability of dolomite. Physicochem Probl Mineral Process https://doi.org/10.37190/ppmp/150702

Arvidson RS, Mackenzie FT (1999) The dolomite problem: control of precipitation kinetics by temperature and saturation state. Am J Sci 299:257–288. https://doi.org/10.2475/ajs.299.4.257

Astilleros JM, Fernandez-Diaz L, Putnis A (2010) The role of magnesium in the growth of calcite: an AFM study. Chem Geol 271:52–58. https://doi.org/10.1016/j.chemgeo.2009.12.011

Baker PA, Kastner M (1981) Constraints on the formation of sedimentary dolomite. Science 213:214–216

Brady PV, Krumhansl JL, Papenguth HW (1996) Surface complexation clues to dolomite growth. Geochim Cosmochim Acta 60:727–731

Braissant O, Decho AW, Dupraz C, Glunk C, Przekop KM, Visscher PT (2007) Exopolymeric substances of sulfate-reducing bacteria: interactions with calcium at alkaline pH and implication for formation of carbonate minerals. Geobiology 5:401–411. https://doi.org/10.1111/j.1472-4669.2007.00117.x

Burgos-Cara A, Putnis CV, Rodriguez-Navarro C, Ruiz-Agudo E (2017) Hydration effects on the stability of calcium carbonate prenucleation species. Minerals https://doi.org/10.3390/min7070126

Burton WK, Cabrera N, Frank FK (1951) The growth of crystals and the equilibrium structure of their surfaces. Philos Trans R Soc Lond 243:299–358

Cai WK, Liu JH, Zhou CH, Keeling J, Glasmacher UA (2021) Structure, genesis and resources efficiency of dolomite: new insights and remaining enigmas. Chem Geol https://doi.org/10.1016/j.chemgeo.2021.120191

Calvet E, Boivinet P, Noel M, Thibon H, Maillard A, Tertian R (1952) Contribution a l'etude des gels d'alumine. Bull Soc Chim Fr 19:99–108

Casado AI, Alonso-Zarza AM, La Iglesia A (2014) Morphology and origin of dolomite in paleosols and lacustrine sequences. Examples from the Miocene of the Madrid Basin. Sed Geol 312:50–62. https://doi.org/10.1016/j.sedgeo.2014.07.005

Deelman JC (1999) Low-temperature nucleation of magnesite and dolomite. Neues Jb Miner Monat 289–302

Deng SC, Dong HL, Lv G, Jiang HC, Yu BS, Bishop ME (2010) Microbial dolomite precipitation using sulfate reducing and halophilic bacteria: results from Qinghai Lake, Tibetan Plateau, NW China. Chem Geol 278:151–159. https://doi.org/10.1016/j.chemgeo.2010.09.008

Di Lorenzo F, Burgos-Cara A, Ruiz-Agudo E, Putnis CV, Prieto M (2017) Effect of ferrous iron on the nucleation and growth of CaCO3 in slightly basic aqueous solutions. CrystEngComm 19:447–460. https://doi.org/10.1039/c6ce02290a

Diaz-Hernandez JL, Sanchez-Navas A, Reyes E (2013) Isotopic evidence for dolomite formation in soils. Chem Geol 347:20–33. https://doi.org/10.1016/j.chemgeo.2013.03.018

dos Anjos APA, Sifeddine A, Sanders CJ, Patchineelam SR (2011) Synthesis of magnesite at low temperature. Carbonate Evaporite 26:213–215. https://doi.org/10.1007/s13146-011-0063-4

Eiblmeier J, Kellermeier M, Rengstl D, Garcia-Ruiz JM, Kunz W (2013) Effect of bulk pH and supersaturation on the growth behavior of silica biomorphs in alkaline solutions. CrystEngComm 15:43–53. https://doi.org/10.1039/c2ce26132d

Fussmann D, von Hoyningen-Huene AJE, Reimer A, Schneider D, Babkova H, Peticzka R, Maier A, Arp G, Daniel R, Meister P (2020) Authigenic formation of Ca-Mg carbonates in the shallow alkaline Lake Neusiedl, Austria. Biogeosciences 17:2085–2106. https://doi.org/10.5194/bg-17-2085-2020

Gachuz-Muro H, Sohrabi M, Benavente D (2017) Dissolution of rock during smart water injection in heavy oil carbonate reservoirs by natural generation of acidic water. Energy Fuels 31:11852–11865. https://doi.org/10.1021/acs.energyfuels.7b02163

Garcia-Ruiz JM, Melero-Garcia E, Hyde ST (2009) Morphogenesis of self-assembled nanocrystalline materials of barium carbonate and silica. Science 323:362–365. https://doi.org/10.1126/science.1165349

Hakim SS, Olsson MHM, Sorensen HO, Bovet N, Bohr J, Feidenhans'l R, Stipp SLS (2017) Interactions of the Calcite {10.4} Surface with Organic Compounds: Structure and Behaviour at Mineral—organic Interfaces. Sci Rep https://doi.org/10.1038/s41598-017-06977-4

Ishihara S, Sahoo P, Deguchi K, Ohki S, Tansho M, Shimizu T, Labuta J, Hill JP, Ariga K, Watanabe K, Yamauchi Y, Suehara S, Iyi N (2013) Dynamic breathing of CO2 by hydrotalcite. J Am Chem Soc 135:18040–18043

Ji YK, Madhav D, Vandeginste V (2022) Kinetics of enhanced magnesium carbonate formation for CO2 storage via mineralization at 200 degrees C. Int J Greenhouse Gas Control https://doi.org/10.1016/j.ijggc.2022.103777

Kaczmarek SE, Sibley DF (2011) On the evolution of dolomite stoichiometry and cation order during high-temperature synthesis experiments: an alternative model for the geochemical evolution of natural dolomites. Sed Geol 240:30–40

King HE, Satoh H, Tsukamoto K, Putnis A (2013) Nanoscale observations of magnesite growth in chloride- and sulfate-rich solutions. Environ Sci Technol 47:8684–8691. https://doi.org/10.1021/es401188j

Kuma R, Hasegawa H, Yamamoto K, Yoshida H, Whiteside JH, Katsuta N, Ikeda M (2019) Biogenically induced bedded chert formation in the alkaline palaeolake of the Green River Formation. Sci Rep https://doi.org/10.1038/s41598-019-52862-7

Li FB, Teng FZ, Chen JT, Huang KJ, Wang SJ, Lang XG, Ma HR, Peng YB, Shen B (2016) Constraining ribbon rock dolomitization by Mg isotopes: implications for the "dolomite problem." Chem Geol 445:208–220. https://doi.org/10.1016/j.chemgeo.2016.06.003

Liebermann O (1967) Synthesis of dolomite. Nature 213:241–+. https://doi.org/10.1038/213241a0

Liu D, Xu YY, Papineau D, Yu N, Fan QG, Qiu X, Wang HM (2019) Experimental evidence for abiotic formation of low-temperature proto-dolomite facilitated by clay minerals. Geochim Cosmochim Ac 247:83–95. https://doi.org/10.1016/j.gca.2018.12.036

Ma JY, Xie SY, Liu D, Carranza EJM, He ZL, Zhang MH, Wang TY (2021) Effects of Fe(3+)on dissolution dynamics of carbonate rocks in a shallow burial reservoir. Nat Resour Res 30:1291–1303. https://doi.org/10.1007/s11053-020-09765-6

Martinez RE, Weber S, Grimm C (2016) Effects of freshwater Synechococcus sp cyanobacteria pH buffering on CaCO3 precipitation: implications for CO2 sequestration. Appl Geochem 75:76–89. https://doi.org/10.1016/j.apgeochem.2016.10.017

Mather CC, Lampinen HM, Tucker M, Leopold M, Dogramaci S, Raven M, Gilkes RJ (2023) Microbial influence on dolomite and authigenic clay mineralisation in dolocrete profiles of NW Australia. Geobiology. https://doi.org/10.1111/gbi.12555

McCormack J, Bontognali TRR, Immenhauser A, Kwiecien O (2018) Controls on cyclic formation of quaternary early diagenetic

dolomite. Geophys Res Lett 45:3625–3634. https://doi.org/10.1002/2018gl077344
McHargue TR, Price RC (1982) Dolomite from clay in argillaceous or shale-associated marine carbonates. J Sediment Petrol 52:873–886
Meister P (2014) Two opposing effects of sulfate reduction on carbonate precipitation in normal marine, hypersaline, and alkaline environments Reply. Geology 42:E315–E315. https://doi.org/10.1130/g35240y.1
Meister P, Reyes C, Beaumont W, Rincon M, Collins L, Berelson W, Stott L, Corsetti F, Nealson KH (2011) Calcium and magnesium-limited dolomite precipitation at Deep Springs Lake, California. Sedimentology 58:1810–1830. https://doi.org/10.1111/j.1365-3091.2011.01240.x
Meister P, Frisia S, Dodony I, Pekker P, Molnar Z, Neuhuber S, Gier S, Kovacs I, Demeny A, Posfai M (2023) Nanoscale pathway of modern dolomite formation in a shallow, Alkaline Lake. Cryst Growth Des 23:3202–3212. https://doi.org/10.1021/acs.cgd.2c01393
Moghaddam SZ, Thormann E (2019) The Hofmeister series: specific ion effects in aqueous polymer solutions. J Colloid Interf Sci 555:615–635. https://doi.org/10.1016/j.jcis.2019.07.067
Mohammed I, Al Shehri D, Mahmoud M, Kamal MS, Arif M, Alade OS, Patil S (2022) Investigation of surface charge at the mineral/brine interface: implications for wettability alteration. Front Mater https://doi.org/10.3389/fmats.2022.891455
Moreira NF, Walter LM, Vasconcelos C, McKenzie JA, McCall PJ (2004) Role of sulfide oxidation in dolomitization: sediment and pore-water geochemistry of a modern hypersaline lagoon system. Geology 32:701–704. https://doi.org/10.1130/g20353.1
Palandri JL, Kharaka YK (2004) A compilation of rate parameters of water-mineral interaction kinetics for application to geochemical modeling. In: Survey UG (ed), Water Resources Investigations Report
Parkhurst DL (1995) User's guide to PHREEQC: a computer program for speciation, reaction-path, advective-transport, and inverse geochemical calculations. In: Center ESI (ed), Open File Reports Section. US Geological Survey, Lakewood, Colorado
Petrash DA, Bialik OM, Bontognali TRR, Vasconcelos C, Roberts JA, McKenzie JA, Konhauser KO (2017) Microbially catalyzed dolomite formation: from near-surface to burial. Earth-Sci Rev 171:558–582. https://doi.org/10.1016/j.earscirev.2017.06.015
Pham VTH, Lu P, Aagaard P, Zhu C, Hellevang H (2011) On the potential of CO2-water-rock interactions for CO2 storage using a modified kinetic model. Int J Greenhouse Gas Control 5:1002–1015. https://doi.org/10.1016/j.ijggc.2010.12.002
Pokrovsky OS, Schott J, Thomas F (1999) Dolomite surface speciation and reactivity in aquatic systems. Geochim Cosmochim Ac 63:3133–3143. https://doi.org/10.1016/s0016-7037(99)00240-9
Pokrovsky OS, Golubev SV, Schott J (2005) Dissolution kinetics of calcite, dolomite and magnesite at 25 degrees C and 0 to 50 atm pCO(2). Chem Geol 217:239–255. https://doi.org/10.1016/j.chemgeo.2004.12.012
Roberts JA, Kenward PA, Fowle DA, Goldstein RH, Gonzalez LA, Moore DS (2013) Surface chemistry allows for abiotic precipitation of dolomite at low temperature. Proc Natl Acad Sci USA 110:14540–14545. https://doi.org/10.1073/pnas.1305403110
Rodriguez-Blanco JD, Shaw S, Benning LG (2015) A route for the direct crystallization of dolomite. Am Miner 100:1172–1181
Ruiz-Agudo E, Putnis CV (2012) Direct observations of mineral-fluid reactions using atomic force microscopy: the specific example of calcite. Mineral Mag 76:227–253. https://doi.org/10.1180/minmag.2012.076.1.227
Ruiz-Agudo E, Putnis CV, Rodriguez-Navarro C, Putnis A (2011a) Effect of pH on calcite growth at constant a(Ca2+)/a(CO32-) ratio and supersaturation. Geochim Cosmochim Ac 75:284–296. https://doi.org/10.1016/j.gca.2010.09.034
Ruiz-Agudo E, Urosevic M, Putnis CV, Rodriguez-Navarro C, Cardell C, Putnis A (2011b) Ion-specific effects on the kinetics of mineral dissolution. Chem Geol 281:364–371. https://doi.org/10.1016/j.chemgeo.2011.01.003
Safavi MS, Masihi M, Safekordi AA, Ayatollahi S, Sadeghnejad S (2020) Effect of SO4-2 ion exchanges and initial water saturation on low salinity water flooding (LSWF) in the dolomite reservoir rocks. J Dispersion Sci Technol 41:841–855. https://doi.org/10.1080/01932691.2019.1614026
Sanati A, Malayeri MR, Busse O, Weigand JJ, Beckmann M (2022) Surface energy and wetting behavior of dolomite in the presence of carboxylic acid-based deep eutectic solvents. Langmuir 38:15622–15631. https://doi.org/10.1021/acs.langmuir.2c02312
Santos PS, Coelho ACV, Santos HS, Kiyohara PK (2009) Hydrothermal synthesis of well-crystallised boehmite crystals of various shapes. Mater Res 12:437–445
Sibley DF, Dedoes RE, Bartlett TR (1987) Kinetics of dolomitization. Geology 15:1112–1114
Tao Q, Zeng Q, Chen M, He H, Komareni S (2019) Formation of saponite by hydrothermal alteration of metal oxide: implication for the rarity of hydrotalcite. Am Miner 104:1156–1164
Vandeginste V, Snell O, Hall MR, Steer E, Vandeginste A (2019) Acceleration of dolomitization by zinc in saline waters. Nat Commun https://doi.org/10.1038/s41467-019-09870-y
Vandeginste V (2021) Effect of pH cycling and zinc ions on calcium and magnesium carbonate formation in saline fluids at low temperature. Minerals https://doi.org/10.3390/min11070723
Wanas HA, Sallam E (2016) Abiotically-formed, primary dolomite in the mid-Eocene lacustrine succession at Gebel El-Goza El-Hamra, NE Egypt: an approach to the role of smectitic clays. Sed Geol 343:132–140. https://doi.org/10.1016/j.sedgeo.2016.08.003
Wang HL, Liu HB, Xie JJ, Li HW, Chen TH, Chen P, Chen D (2017) An insight into the carbonation of calcined clayey dolomite and its performance to remove Cd (II). Appl Clay Sci 150:63–70. https://doi.org/10.1016/j.clay.2017.09.012
Wang X, Xu XX, Ye Y, Wang C, Liu D, Shi XC, Wang S, Zhu X (2019) In-situ High-Temperature XRD and FTIR for calcite, dolomite and magnesite: an harmonic contribution to the thermodynamic properties. J Earth Sci 30:964–976. https://doi.org/10.1007/s12583-019-1236-7
Wang JJ, Zhao YY, Li D, Qi PL, Gao X, Guo N, Meng RR, Tucker ME, Yan HX, Han ZZ (2022) Extreme halophilic bacteria promote the surface dolomitization of calcite crystals in solutions with various magnesium concentrations. Chem Geol https://doi.org/10.1016/j.chemgeo.2022.120998
Warren J (2000) Dolomite: occurrence, evolution and economically important associations. Earth-Sci Rev 52:1–81. https://doi.org/10.1016/s0012-8252(00)00022-2
Wen YZ, Sanchez-Roman M, Li YL, Wang CS, Han ZP, Zhang LM, Gao Y (2020) Nucleation and stabilization of Eocene dolomite in evaporative lacustrine deposits from central Tibetan plateau. Sedimentology 67:3333–3354. https://doi.org/10.1111/sed.12744
Wilkinson JJ (2010) A review of fluid inclusion constraints on mineralization in the Irish ore field and implications for the genesis of sediment-hosted Zn-Pb deposits. Econ Geol 105:417–442. https://doi.org/10.2113/gsecongeo.105.2.417
Xia F, Brugger J, Chen GR, Ngothai Y, O'Neill B, Putnis A, Pring A (2009) Mechanism and kinetics of pseudomorphic mineral replacement reactions: a case study of the replacement of pentlandite by violarite. Geochim Cosmochim Acta 73:1945–1969. https://doi.org/10.1016/j.gca.2009.01.007
Xu M, Sullivan K, VanNess G, Knauss KG, Higgins SR (2013) Dissolution kinetics and mechanisms at dolomite-water interfaces: effects of electrolyte specific ionic strength. Environ Sci Technol 47:110–118. https://doi.org/10.1021/es301284h

Yang F, Wang Q, Yan J, Fang J, Zhao J, Shen W (2012) Preparation of high pore volume pseudoboehmite doped with transition metal ions through direct precipitation method. Ind Eng Chem Res 51:15386–15392

Yang ZL, Liu XS, Han X, Zhou H, Zhan S, Gui XJ, Niu JH, Wang K (2022) Multiple-stage injection of deep hydrothermal fluids in the dolostone reservoirs of ordovician majiagou formation, southern ordos basin. Front Earth Sci https://doi.org/10.3389/feart.2022.954192